Civil Engineering Infrastructures Journal xx,xx
DOI: 10.22059/CEIJ.2023.353447.1903

Comparative study of the effects of key factors on concrete-to-concrete bond strength

Vahag Mack[a], Reza Salehfard[a], Asghar Habibnejad Korayem[a*]

(a) School of Civil Engineering, Iran University of Science and Technology (IUST), Tehran, Iran

(*) corresponding author: ahkorayem@iust.ac.ir

Received: 09/01/2023
Revised: 19/04/2023
Accepted: 20/05/2023

Abstract

This study aims to investigate the effects of key parameters on the interfacial bond strength between two concrete members. Different types of overlay in terms of strength (normal-strength concrete, high-strength concrete), surface roughness, and adhesive type were considered as variable factors influencing the bond behavior. First, the surface roughness of the old concrete and the compressive strength of the concrete overlay were evaluated separately, and then among the specimens, the composite with the highest bond strength was chosen as the optimum concrete composite. After finding the optimum composite, epoxy adhesive and cellulose mortar were applied to the optimum sample, and its corresponding interfacial strength was evaluated by bi-

surface shear and splitting tensile strength tests. The results showed that, as the compressive strength of new concrete and concrete roughness increases, the bond strength increases. The highest bond strength achieved in composites containing high-strength concrete was 23.37% higher than that of samples with normal-strength concrete. Moreover, the interfacial bond strength of composite with the wire-brushed surface was the highest among other treatment methods, due to the interlocking action it provides. The bond strength of concrete composites containing epoxy adhesive was ~100-200% higher than that of samples without epoxy resin. However, the addition of cellulose mortar slightly reduced the adhesion resistance of the optimum sample. Therefore, it is anticipated that the use of high-strength concrete concomitant with wire-brushed surface treatment and epoxy resin adhesive shows substantial potential as an excellent method for repair of concrete structure.

Keywords: concrete repair, High-strength-concrete, interfacial strength, surface preparation, adhesive agent

1. Introduction

Concrete structures can undergo intense forces during construction for a variety of reasons. These forces can impose maximum stress on a concrete structure, causing cracks and, finally, failure of that member (Zhou et al. 2008). The construction budget used for maintenance and repair of structures in the US is estimated at $18–21 billion per year (Du et al. 2019). Therefore, the safe and reliable design of repair materials is vital. It relies heavily on the availability of validated engineering materials and necessitates standardized quality improvement measures based on the constituents and mix design of the repair material.

Adding new concrete to old concrete or replacing new concrete with damaged

concrete is one of the essential methods in repairing and strengthening concrete structures (EL Afandi et al. 2023; Behforouz et al. 2023). This procedure produces concrete-to-concrete interfaces with distinct properties. The interface plays a vital role in concrete-to-concrete bond strength. Therefore, the new concrete must have good adhesion to the old concrete substrate (Ezoddin et al. 2020; Jafarinejad et al. 2019; Al-Osta et al. 2022). However, consequence of insufficient bonding may cause a decrease in bond strength between composites (Austin et al. 1995). It has been represented that extreme interfacial roughness may further restrain the overlay shrinkage, causing higher tensile and shear stresses on the overlay and interface, which increases the probability of overlay cracking or interface detachment (Zhou et al. 2008). In general, there are three different types of concrete-to-concrete interfaces. One includes when a new concrete overlay is placed against a concrete substrate (hardened concrete). This process is common in renovating damaged concrete structures such as concrete jacketing, precast connections, and ground support in tunnel operations. Placing hardened concrete against hardened concrete is another example of a concrete-to-concrete interface common in precast structures, such as bridge decks made of post-tension/pre-stressed concrete members. Eventually, adding concrete overlay on fresh concrete is widely used in additive manufacturing and digital fabrication, such as 3D concrete printing (Babafemi et al. 2021).

Factors that affect the bond strength (Santos et al. 2012; Momayez et al. 2005; Julio et al. 2006; He et al. 2017; Julio et al. 2004; Daneshvar et al. 2022; Baharuddin et al. 2020) include the type and mechanical properties of both old and new concrete (compressive strength, young's modulus, age, and curing condition) (Julio et al. 2006; Huang et al. 2019), substrate roughness, and

moisture condition (Santos et al. 2012; Piotrowski and Garbacz, 2014; Zhou et al. 2008; Beushausen et al. 2017), the environmental conditions (temperature, freeze-thaw cycles, etc.) (Çolaket et al. 2009), the use of interface adhesion agents (type, thickness, casting and curing conditions) (Huang et al. 2019; Valikhani et al. 2020; Guo et al. 2018), and finally methods being used to measure the interfacial strength between new and old concrete (Feng et al. 2020; Farzad et al. 2019). Many studies have focused on the interfacial bond strengths of concrete-concrete composites by considering overlays with different types and strength properties (Al-Madani et al. 2022; Prado et al. 2022; Feng et al. 2022). Julio et al. (2006) studied the influence of added concrete compressive strength on bond strength between concrete prisms. They used three different concrete mixtures with compressive strength of 30, 50, and 100 MPa for the added concrete. They noticed an increment of bond strength in shear with the increase of added concrete compressive strength. Mangat and Flaherty (2000) investigated feasibility of using two materials for repairing highway bridges. One of the materials had low stiffness relative to the substrate and the other one had higher stiffness. Their results showed that using relatively stiff materials displayed efficient structural interaction with the subtrate. In another study, Zhou et al. (2008) conducted an experiment to assess the impact of the elastic modulus of concrete overlay on bond strength. Their findings indicated that repair materials with higher mechanical properties exhibit superior bond strength.

Carbonell et al. (2014) and Valipour et al (2020) evaluated the interfacial bond performance between ultra-high performance concrete (UHPC) overlay and normal-strength concrete (NSC). It was deduced that regardless of other involved parameters and applied loads, the bond strengths between

two concretes were strong enough when UHPC was used. Tayeh et al. (2012) assessed the permeability characteristics of the UHPC-NSC interface using water, gas, and rapid chloride permeability (RCP) tests. Prado et al. (2022) revealed that high-strength concrete (HSC)-UHPC interface represented a bond strength similar or superior to that of the monolithic HSC specimen. In another study, the effects of bond properties of light-weight concrete (LWC)-normal weight concrete (NWC) were evaluated by considering different parameters (strength grade, interface roughness, use of steel fiber, etc.) (Huang et al. 2019). It is reported that the selection of interfacial agents (epoxy resin, cement paste, polymer binder, etc.) has a considerable effect on the bond strength between the new and old concretes (Shin and Lange 2012). He et al. (2017) pointed out that different types of bonding agents have different efficiency and may lead to a different degree of increase in mechanical performance. Moreover, the use of bonding agents significantly affects failure types (Courard et al. 2014). Nevertheless, the advantages of the use of bonding agents are not approved by all the researchers. Some researchers asserted that the application of a bonding agent leads to the formation of an extra plane contributing to the decrement of effective interlocking between substrate and overlay concrete (Julio et al. 2004). Valikhani et al. (2020) reported that the application of a bonding agent could be harmful to the strength of the bond between new and old concrete. Several surface preparation techniques have been utilized by researchers, namely wire-brushing, shot blasting, grinding, sand-water blasting, water jetting, chipping, pneumatic hammer, milling, and hydro-demolition (Diab et al. 2017; Gadri and Guettala, 2017). Santos et al. (2012) and Valikhani et al. (2020) demonstrated that the sand-blasting method could be used as the best interface

preparation technique to get the highest bonding strength. Whilst, it is envisaged that some methods, such as pneumatic hammer, are harmful to the concrete interface since this method causes micro-cracks in the concrete substrate. It is still under debate how interface bonding strength is affected by the roughness (Santos et al. 2012; Julio et al. 2004). HSC is designed to have better mechanical performances and greater resistance to aggressive chemicals than normal concrete (Tu et al. 2006). HSC possesses high strength and less inhomogeneity and micro-cracks at the interfacial transition zone (ITZ). Therefore, it is being paid more attention to and can be used to repair and strengthen the damaged concrete owing to its excellent mechanical properties (Dybeł and Wałach, 2017). A quantitative definition of HSC is impossible for an engineer since it is relative and depends on time and location (Nawy 2000). In North American and Canadian codes (Nawy 2000; ACI 213R-87), concrete has a 28-day compressive strength of at least 41MPa and is regarded as HSC. On the other hand, the FIP/CEB code (de la Precontrainte 1983) describes HSC as concrete, having a minimum 28-day compressive strength of 60 MPa. In light of the previous discussion, the purpose of this study is to evaluate the bonding strength behavior between NC or HSC as an overlay and NC as a substrate layer. Three different surface-preparation methods were used to elaborate the interfacial bond strength. The bond strength was measured through bi-surface and tensile splitting tests. The highest bond strength obtained by considering the above parameters was selected as the optimum specimen. Afterwards, two types of adhesive agents, namely epoxy resin and hydroxyethyl methylcellulose (HEMC) powder, were also applied to the optimum concrete sample substrate, and the conclusions were made.

2. Experimental program

2.1. Materials

2.1.1. Concrete

The adopted concrete mixtures for NSC and HSC were set to achieve 28-day compressive strengths of 40 MPa and 70 MPa, respectively. The aggregates used in the mix design were fine sand, coarse sand, and coarse limestone. The maximum aggregate size in the mix design of normal and high-strength concrete was chosen, 19 mm. Aggregates used in the mix design were fine sand with most particles passing through a 4.75-mm sieve, and coarse limestone with mostly rounded shape. The Finesses modulus of aggregates was obtained at 5.46 according to the Fuller-Thompson curve (Xu and Hao, 2012). The physical and chemical compositions of cement and silica fume used in NSC and HSC are shown in Table 1. A carboxylic-based superplasticizer (SP) was also concluded in the mix design of silica fume concrete to obtain a concrete with a workability and slump according to the normal-strength concrete. The details can be found in Table 2. The optimum mixtures for both normal and high-strength concrete were designed and modified to meet the desired compressive strength and workability for both normal-strength and high-strength concrete. The concrete mix proportions are listed in Table 3. The amount of water for both concretes was chosen, 180kg/m^3. Silica-fume used in high-strength concrete was 10% per unit weight of cement.

Table 1. The constituents of cementitious materials.

Chemical composition (%)		
Chemical ingredient	Portland cement	Silica fume
CaO	63.0	0.45
SiO_2	19.42	88.71
Al_2O_3	3.63	0.43
Fe_2O_3	3.23	1.52
SO_3	6.79	0.46
MgO	2.69	0.46
Physical properties		
Specific gravity	3.12	2.3
Specific surface (m^2/gr)	0.3464	17.13

Table 2. Properties of superplasticizer.

Color	Light brown
PH	7
Specific weight (kg/L)	1.03
Chemical base	Poly-carboxylic ether

Table 3. Concrete mixture design.

Concrete	Cement (kg/m^3)	W/B	Gravel (kg/m^3)	Sand (kg/m^3)	Silica fume (kg/m^3)	SP (% unit weight of cement)
NSC	360	0.5	1066	686	-	-
HSC	467	0.35	983	632	47	0.3 %

2.1.2. Epoxy resin

Epoxy-based resins are the most generally used adhesives in bonded concrete composites, which enhance the interfacial zone and alter the bond strength and failure modes of the produced composites (Baloch et al. 2021). The efficiency of epoxy resin is highly attributed to its curing conditions and thickness (Michels et al. 2016). In this study, an epoxy resin under the brand name Araldite 420 was used as the bonding agent between concrete materials, known as the most common commercial resin epoxies widely used in reinforcing civil structures. The epoxy is DGEBA (diglicidyl ether of Bisphenol A) based, supplied by Huntsman Company, Australia, and the hardener was Trioxatridecanediamine. This epoxy was chosen due to its higher strength, less viscosity, and less elongation at breakage. The chemical formula of epoxy adhesive is shown in Fig. 1. The physical properties of resin, hardener, and the mixture can be found in Table 4.

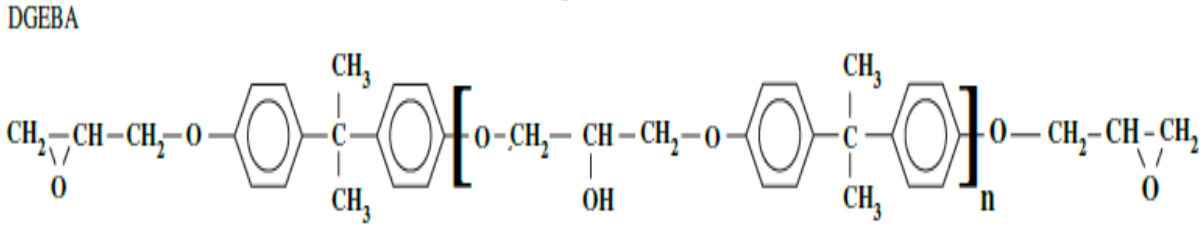

Fig. 1. DGEBA epoxy resin chemical formulae (Delor-Jestin et al. 2006).

Table 4. The physical properties of epoxy adhesive and its constituents.

Property	Araldite 420 A	Araldite 420 B	Mixed adhesive
Color	Yellow	blue	Dark green
Specific gravity	1.2	1.0	Approx. 1.1
Viscosity at 25°C (Pa. s)	100-300	0.6-1.4	35-45

Young's modulus (MPa)	-	-	1495
Tensile strength (MPa)	-	-	29

The powder used in order to increase the adhesion between the concrete layers was cellulose-based, known as hydroxyethyl methylcellulose (HEMC). This powder is a multifunctional additive for construction materials, especially dry-mix products. It can improve the workability of both cement-based and gypsum-based materials by extending open time and enhancing adhesion, lubricity, shrink and crack resistance. They are primarily used in tile adhesive, plasters, render finishes, and exterior insulation systems. Fig. 2a shows the chemical formulae of the HEMC powder used in the mortar, and Fig. 2b demonstrates the white HEMC powder as a dry product. The physical and chemical properties of HEMC powder are according to Table 5.

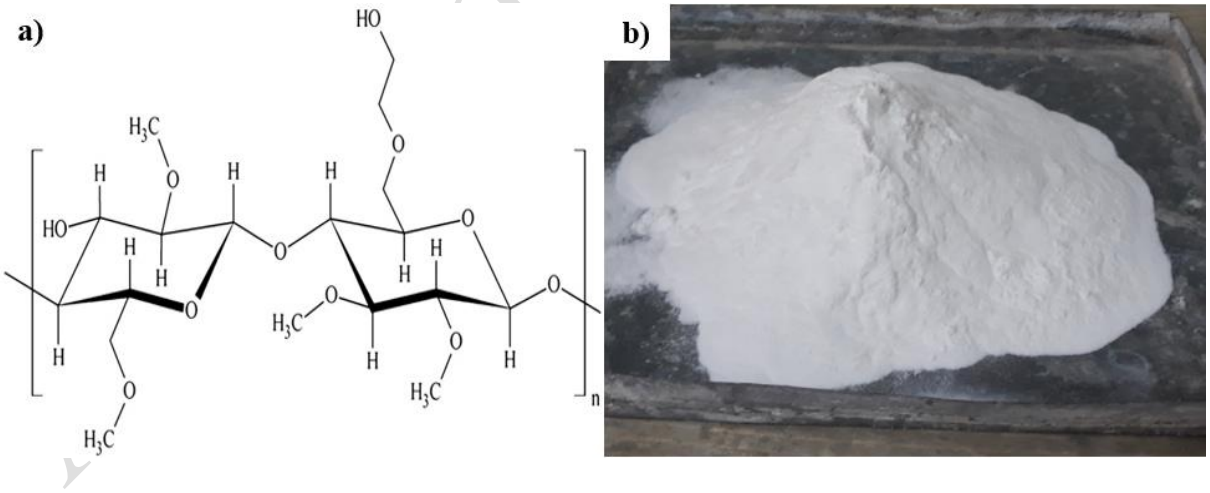

Fig . 2. (a) Chemical formulae of powder adhesive (Bülichen et al. 2012); (b) the white HEMC powder adhesive.

Table 5. The physical and chemical properties of HEMC powder adhesive.

Appearance	White to cream-colored powered	pH value	5-8
Bulk density	0.3-0.6 g/cm^3	Residue on ignition	5.0 max
Particle size	99% <180 µm	Brookfield viscosity (mPa.s) (2% solution 20-25 c)	40000-55000
Moisture (%)	5.0 max	NDJ viscosity (mPa.s) (2% solution 20-25 c)	90000-100000

2.2. Test methods

2.2.1. Compressive strength test

Compressive strength tests were performed in order to classify the materials to ensure that the chosen concrete materials satisfied the strength criteria set out earlier. The tests were carried out on concrete cubes measuring 150 mm, following standard procedures in BS EN-12390 (EN 2009). The specimens were tested when both NSC and HSC reached 28-days of age. Three compression tests were conducted on concrete composites. The cubic specimens were loaded according to BS EN-12390 (EN 2009). Constant rate of loading within the range 0.4-0.8 MPa/s was applied and then increased continuously until no greater load can be sustained. The compressive strength was calculated using Eq. 1, where f_c is the compressive strength (MPa), F is the maximum load at failure (N) and A_c is the cross section of the specimen (mm^2).

$$f_c = \frac{F}{A_c} \quad (1)$$

2.2.2. Splitting tensile and bi-surface tests

The bond strength between the normal and high-strength concrete was examined using

splitting tensile and bi-surface shear tests. A universal testing machine (UTM) with a capacity of 2000 KN was used to apply the load to the test specimens in compression and tension. The interfacial tensile strength was evaluated by conducting the splitting tensile test on a 150 mm cubical specimen. The schematic diagram of the bi-surface shear and splitting tensile test is represented in Figs. 3a-3b (Santos et al. 2012; BSI 2000). In the proposed methods, the experimental bond strength can be calculated using the equations Eqs. 2 and Eqs. 3.

$$F_{ct} = \frac{P}{2bd} \quad (2) \qquad F_{ct} = \frac{2P}{\pi bd} \quad (3)$$

where F_{ct} is the tensile splitting strength (MPa); F is the maximum load applied to the specimen until failure (N), L is the length of the specimen, and d is the depth of the specimen. The required loading rate on the testing machine for splitting tensile test was chosen as per BS-EN 12390-6 (BSI 2000). For the bi-surface shear test, constant loading rate of 0.3 MPa/s was applied until composite specimens failed. Cubic specimens with the dimensions of 15×15×15 cm were used for both splitting tensile and bi-surface shear tests. These experimental tests have some advantages compared to other bond tests. For instance, the specimen geometry is similar to the standard cubic specimens, and the same molds can be used to make the concrete composites; besides, all the specimens are tested in a universal testing machine similar to a compression test without the need for specific apparatus. Loads are also applied symmetrically and produce uniform stress along with the interface. For the bi-surface shear test, the substrate concrete and the concrete overlay comprise two-thirds and one-third of the molds, respectively (Fig. 4a). Contrary to the bi-surface shear specimens, for the splitting tensile test, the substrate concrete and the concrete overlay comprise half of the molds (Fig. 4b). First, the concrete substrate was made in the laboratory by a 100-liter mixer capacity and was placed in

lubricated plastic molds. Then, the specimens were kept in a water tank for 28 days to achieve their ultimate strength. After casting, the specimens were placed in plastic molds for the addition of concrete overlay. Where appropriate, the substrate surface was roughened, and epoxy adhesive and HEMC mortar were applied before placing the new concrete. Three composite specimens were cast based on each surface treatment method, compressive strength of the concrete overlay, and the application of binders between the specimens. After casting concrete overlay, the specimens were cured for additional 28 days before testing. In order to prevent moisture loss, the outside surface of the samples was covered by plastic sheets.

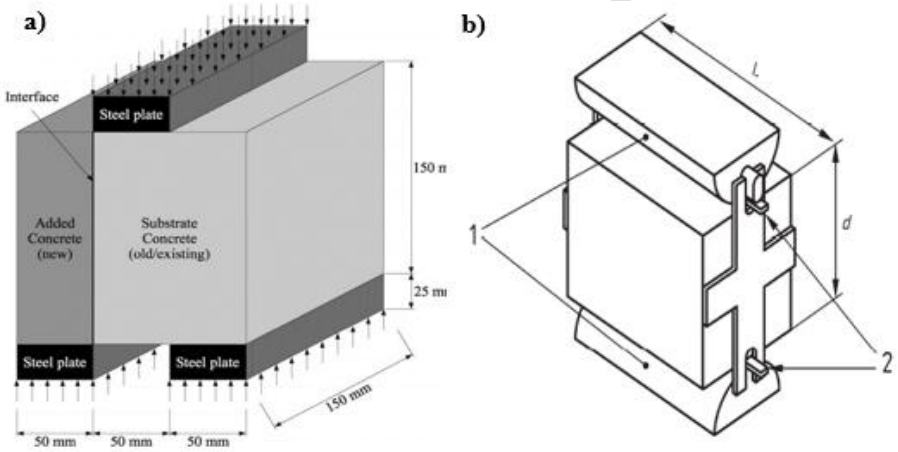

Fig. 3. (a) Bi-surface shear test (Santos et al. 2012); (b) splitting tensile test (BSI 2000).

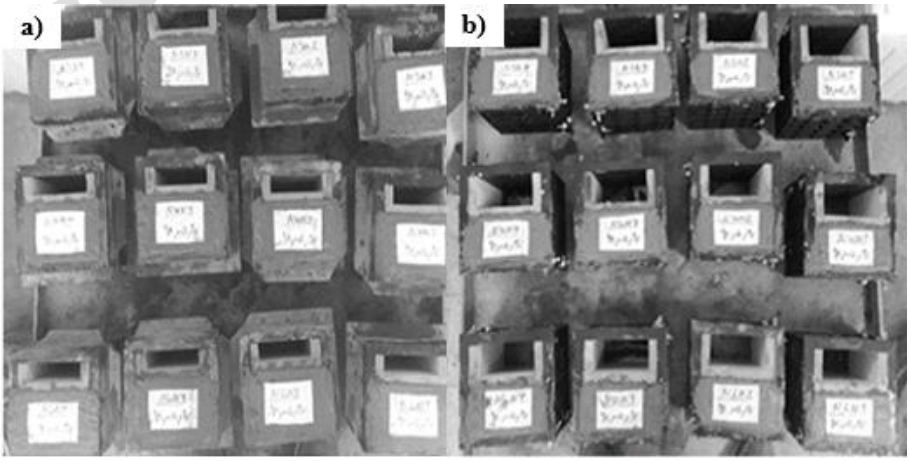

Fig. 4. (a) Tensile splitting samples; (b) bi-surface shear specimens.

2.2.3. Concrete interface treatment

Three different surface roughness were considered in this study, including surface left as cast, surface wire-brushed, and surface partially chipped. The surface preparation methods used were practical and primarily implemented in the construction industry. The term surface left as cast (LAC) in Fig. 5c implies that the concrete overlay was placed directly against the concrete substrate, and no increase in the surface texture of the substrate can be observed. Before placing the concrete overlay, the substrate surface was cleaned with compressed air and a brush to remove any possible dust from the surface. Wire-brushed surface (WB) produces enhanced friction between concrete materials due to revealing some of the substrate aggregates. After the preparation, the surface was once again cleaned with compressed air (Fig. 5a). The third method used for increasing the roughness of the substrate concrete was scrabbling or chipping with a commercial chipping drill (Fig. 5b). This method strikes the surface repeatedly with hardened points to produce momentary mechanical loads that exceed the strength of the concrete, causing it to fracture.

2.2.4. Application of bonding agent

After the concrete surface treatment, the epoxy adhesive and HEMC mortar were applied to concrete surfaces immediately before adding a concrete overlay. The specifications for mixing and preparation of epoxy adhesive and mortar samples were described by the manufacturer. The water to cement ratio was chosen 0.5, and HEMC powder with an amount of 0.7 %-unit weight of cement was used for HEMC mortar. The mixture design and mechanical properties of reference and HEMC mortars including compressive strength and tensile strength are shown in Table 6. The results showed that the compressive strength of HEMC mortar is lower than reference mortar which can be due to delayed hydration of cement in the mortar

(Pourchez et al. 2006). On the other hand, the tensile strength was higher than that of reference mortar. Approximately 1-2 mm thickness was adopted for epoxy adhesive and was applied via cutter. The intended thickness for the mortar was considered 2-3 mm. The adhesive was then applied to the This spatula was also used to apply the mortar to the hardened concrete specimens. The thicknesses of epoxy bonding agent and HEMC mortar were measured by vernier caliper. The thickness was calculated by subtracting the total thickness (specimen and adhesive) from the specimen's length (150 mm). The uniformities were visually checked and precisely controlled by vernier caliper. After applying the mortar to the surfaces, the mortar was smoothed with a trowel to produce a constant and steady thickness. Then, fresh concrete was prepared and added to the old concrete. The surface of the surface of the hardened specimens by the spatula, and afterwards, new concreting was performed on the hardened concrete.

concrete substrate was moistened using a water sprinkler to remain in a saturated surface-dry condition (SSD) and prevent the absorption of water available in HEMC mortar by the substrate. To reach a proper saturated surface dry state, it is critical to achieve a substrate surface showing no signs of water film. Finally, samples were cured at 100% humidity for seven days and then stored in a water tank for additional 21 days at 50% humidity and room temperature. The humidity inside the water tank was regulated by a hydrometer.

Table 6. The mixture design and mechanical properties of HEMC mortar.

Cement (gr)	Water to cement ratio	Aggregate to cement ratio	SP (% unit weight of cement)	HEMC (% unit weight of cement)

500	0.5	3	0.5	0.7
Compressive strength (MPa)			Tensile strength (MPa)	
Reference mortar		HEMC mortar	Reference mortar	HEMC mortar
31.5		23	1.41	1.94

2.2.5. Interface microscopy

The surface texture of the specimens was examined by optical microscopy (stereo optical microscope) with a magnitude of 20x and scanning electron microscopy (SEM) on the scale of nanometers. Two plates of 25×25 mm were cut per concrete surface profile for each microscope analysis. The specimens prepared for the SEM analysis have been thoroughly dried in the oven for 24h. The epoxy specimens were put in the vacuum machine to facilitate the hardening of epoxy and eliminate bubbles created while mixing the epoxy components. The mesostructured wire-brushed and chipped surfaces obtained from the stereo microscope are shown in Figs. 6a-b. Using the results obtained from the observation of the microstructure with a scanning electron microscope (Figs. 6c-6d), one can conclude that concrete surfaces significantly had different surface textures after various treatments. The aggregates are exposed using the wire-brush technique, which is dominant for bonding old concrete and repair material (Fig. 6a). According to Fig.6c, the surface of the substrate has wave-like irregularities, which can increase the mechanical interlocking and, therefore, friction. Fig. 6b and Fig. 6d depict the chipped surface on macroscopic and microscopic scales, respectively. These

figures indicate that the chipping method causes micro-cracks on the concrete surface.

2.2.6. Specimen identification

All specimens were designated as NXYZ, where: N specifies the substrate concrete (N for the Normal Strength Concrete). (X) Represents the surface texture of the substrate concrete (L for the left as cast, W for Wire-brushed, and S for scrabbling (chipping). (Y) Represents epoxy addition or HEMC mortar on the substrate (Y is ignored-when the specimen is considered adherend free). The letter (Z) Shows the overlay concrete (N for the NSC and H for HSC). Taking the NLH specimen as an example, the first N represents substrate material (NSC), the second H is overlay concrete (HSC), and the character L symbolizes surface texture (Left as cast), and no bonding agent was used between concrete materials. In order to compare concrete to concrete bond strength with the real bond strength (continuous concrete composed of the substrate concrete), it was also decided to conclude them in this research. The comparison aimed to see how much strength the composites need to act as a monolithic material, which indicates proficient bond strength. For continuous concrete (15×15×15 cm), the letters N-BR and N-BI have been used, in which BR stands for Brazilian (splitting) tensile test and BI stands for the bi-surface shear test.

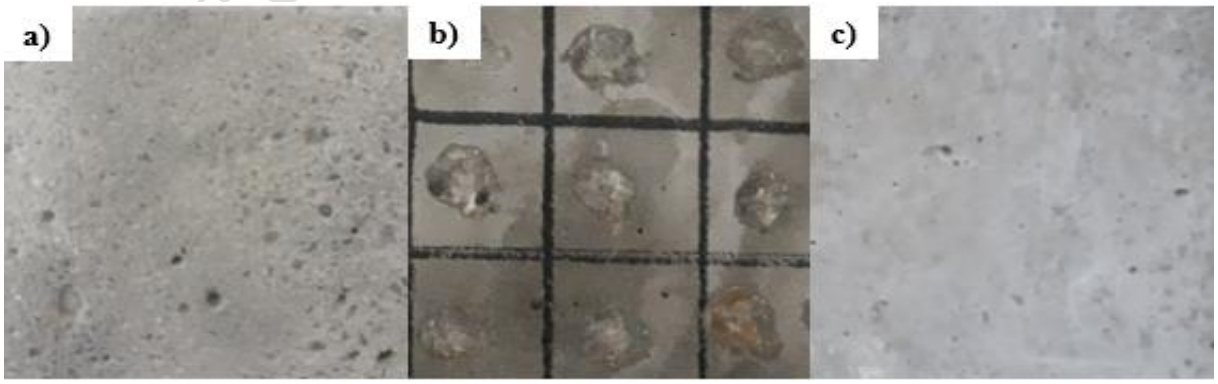

Fig. 5. Surface preparation methods: (a) surface wire brushed; (b) surface partially chipped; (c) surface left as cast.

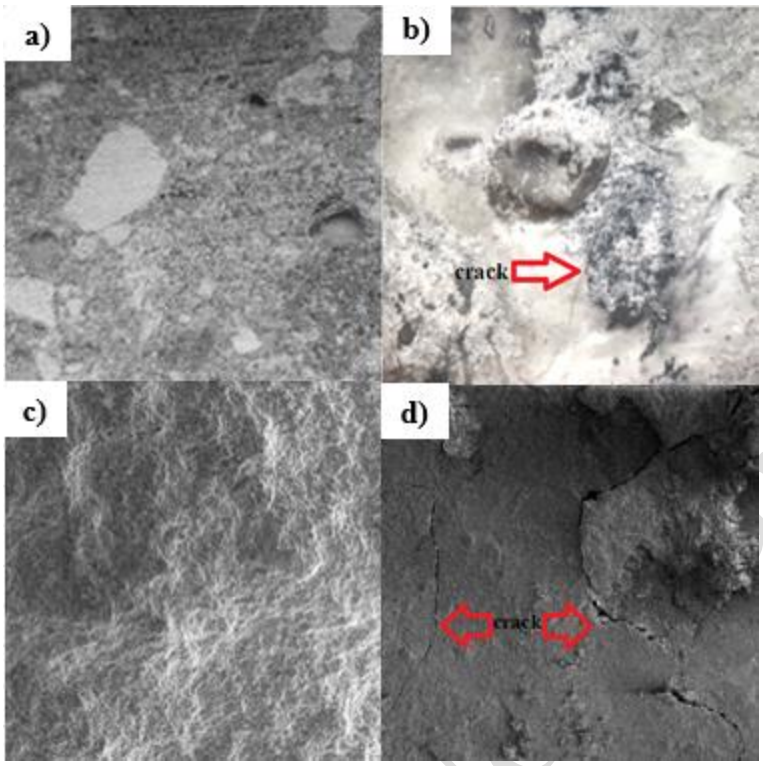

Fig. 6. The microstructure images of new-to-old concrete interface: (a, c) wire-brushed surface; (b, d) chipped surface.

3. Results and discussion

3.1. Compressive strength

The results of the compression test for NSC and HSC concrete are shown in Table 7. The average compressive strength for NSC concrete was 40.12 MPa, which was well matched with the desired compressive strength. The average compressive strength for HSC concrete was 67.75 MPa with a standard deviation of 1.7, which was close to the desired strength. The compressive failures of the specimens are shown in Fig. 7a and Fig. 7b. As illustrated in Fig. 7a, the failure of the normal-strength concrete was non-explosive, contrary to the high-strength concrete, which had an explosive failure (Fig. 7b). The compressive stress-strain curves for both materials are shown in Fig. 7c.

3.2. Evaluation of interfacial bonding strength

3.2.1. The effect of surface treatment

As shown in Fig. 8a, one can see that shear bond strength increases with the increase in the roughness of the concrete substrate. On the other hand, the highest increase in shear among different surface roughness was for the NWN sample.

Table 7. Compressive strength of cubic specimens for both normal strength and high strength concrete as an overlay material.

Concrete composite	Layer	Failure stress (MPa)	Average (MPa)	SD (MPa)	COV (%)
NSC-NSC	Concrete substrate	39.95	40.12	1.96	4.88
		38.26			
		42.17			
	Added concrete	40.9	39.01	2.0	5.12
		39.24			
		36.9			
NSC-NHC	Concrete substrate	38.26	39.23	1.45	3.69
		40.9			
		38.5			
	Added concrete	69.77	67.85	1.7	2.5
		67.30			
		66.50			

Note: SD – standard deviation, COV – coefficient of variance.

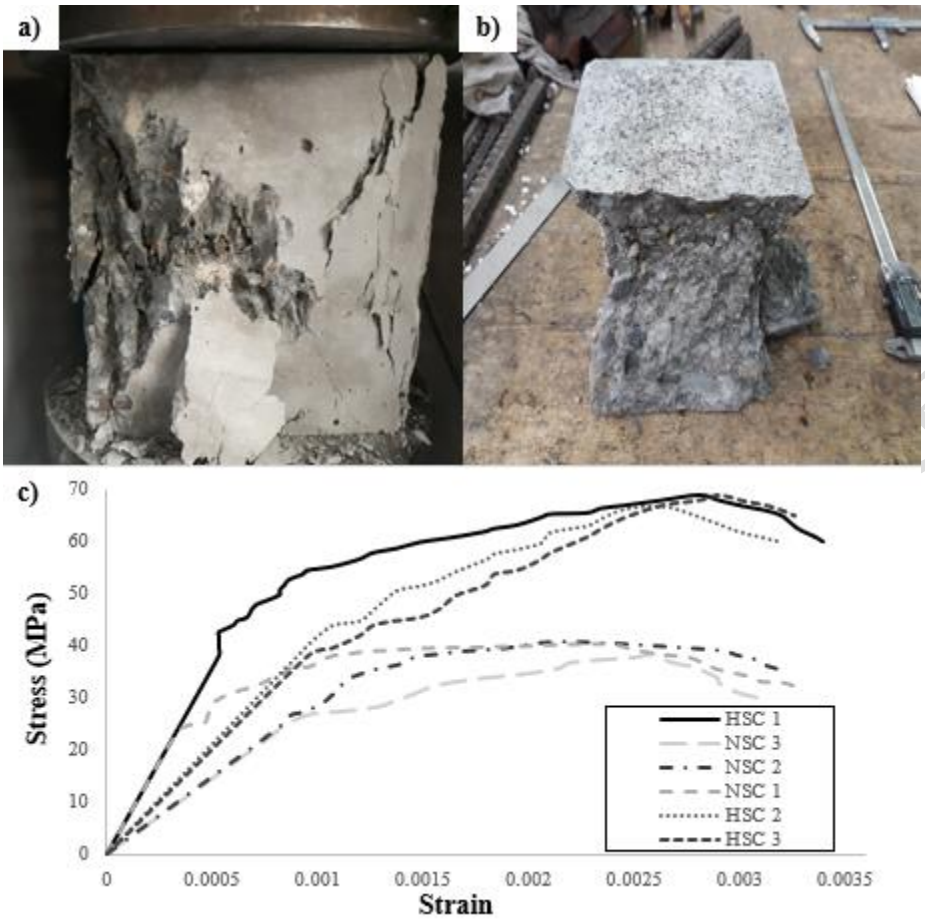

Fig. 7. (a) compressive failure of NSC; (b) compressive failure of HSC; (c) The stress-strain curves obtained from compressive strength tests for of NSC and HSC.

The reason was the manifestation of aggregates outside the surface of the substrate, which increased the friction between the aggregates of the substrate and the cement paste of the fresh concrete. The wire-brushing method increased the friction of aggregates more than other methods of roughening techniques used in this experiment and, as a result, increased the adhesion. As shown in Fig. 8a, the shear resistance of NLN, NWN, and NSN were approximately 12 %, 25 %, and 16 % of shear strength relative to monolithic concrete (Continuous concrete). Lower adhesion resistance of the NSN (chipped sample) can be due to the presence of micro-cracks in old concrete caused by chipping drill, which reduced the adhesion resistance (Fig. 6d).

The highest bond strength obtained from the splitting tensile test was also due to the increased roughness associated with the wire-brushing method (Fig. 8b). The increase in tensile strength of this sample was 1.18 and 1.04 greater than the tensile strength of the left as cast and chipped samples, respectively. As a result, one can conclude that increasing the roughness does not significantly affect the tensile strength. As shown in Fig. 8b, the tensile strength of NLN, NWN, and NSN were approximately 16 %, 19 %, and 18 % of the tensile strength of monolithic concrete.

3.2.2. Influence of overlay strength

The results of the bi-surface shear and splitting tensile tests for concrete composites containing high-strength concrete as an overlay material are shown in Fig. 9a and Fig. 9b. Comparing Fig. 9 with Fig. 8, it can be concluded that among concrete samples, the sample containing high-strength concrete as an overlay achieved the highest value in bond strength. The increased adhesion of concrete composites containing high-strength concrete can be attributed to the role of silica compound of silica fume which generates calcium silicate hydrate (C-S-H) by reacting with calcium hydroxide (Mizan, Ueda, and Matsumoto 2020; Shibao et al. 2019), that corroborates the findings of Momayez et al (Momayez et al. 2005). As shown in Fig. 9a, the shear strength of NLH, NWH, and NSH were approximately 15 %, 28 %, and 20 % of the shear strength of monolithic concrete, respectively. The shear strength of NLH, NWH and NSH samples were 1.23, 1.12, and 1.23 times greater than NLN, NWN, and NSN samples, respectively, which indicated that as the roughness of the substrate increases, the influence of the compressive strength of fresh concrete was reduced. The highest tensile strength among different surface roughness also belonged to the wire-brushed sample, which has a magnitude of 1.35 times greater than the concrete

composite, without any surface roughness. The highest tensile strength was also due to the increased roughness associated with the NWH sample (wire-brushed surface profile and the use of high-strength concrete), which was similar to the shear adhesion resistance. As illustrated in Fig. 9b, the tensile strength of NLH, NWH and NSH samples were approximately 19 %, 26 %, and 23 % of the tensile strength of the monolithic concrete. Therefore, the specimen with the highest shear and tensile strength; that is NWH sample, can be considered as the optimum specimen. The epoxy adhesive and HEMC mortar were added, and further experiments were undertaken.

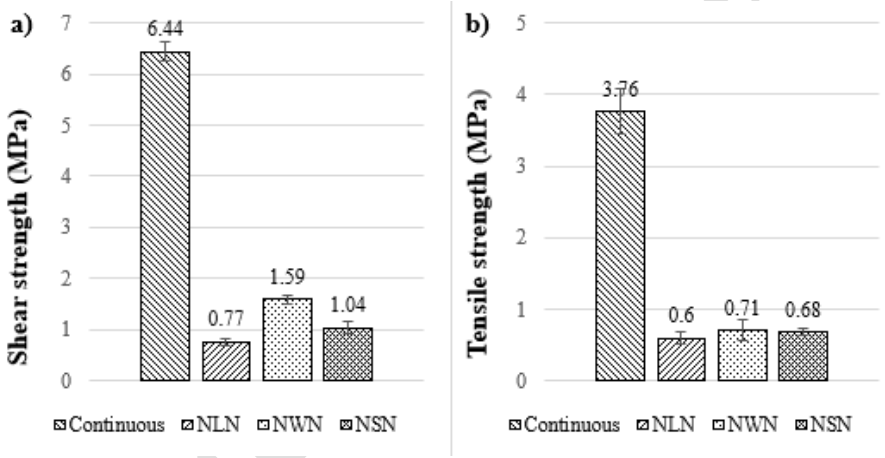

Fig. 8. The interfacial strength of composites with different surface preparations: (a) composites subjected to shear; (b) composites subjected to tension.

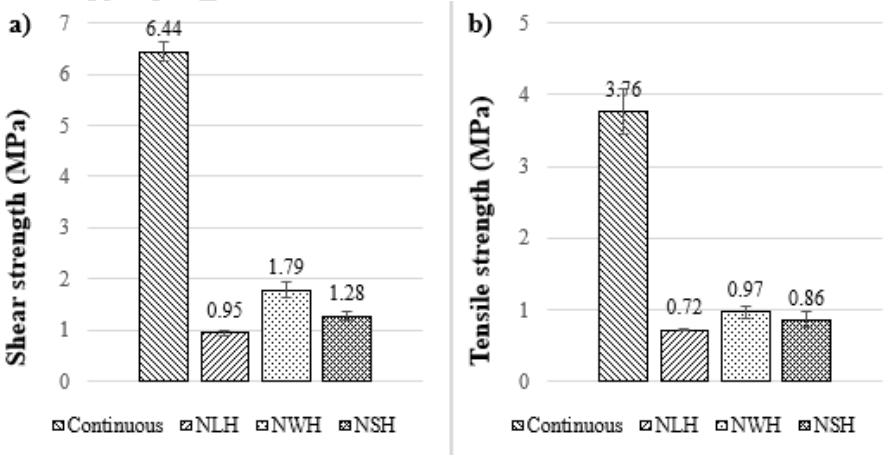

Fig. 9. The interfacial strength of composites containing high-strength concrete as an overlay: (a) composites subjected to shear; (b) composites subjected to tension.

3.2.3. Effect of bonding agent

The bi-surface shear strength of the optimum specimen containing epoxy resin adhesive, as shown in Table 8, was 126% greater than the NWH sample, which indicated the good bonding performance of the adhesive. Comparing Table 8 with Fig. 9a, one can conclude that the shear strength of the epoxy-contained sample was 86.4% of the shear strength of the monolithic concrete. The tensile strength of the optimum specimen with epoxy resin binder showed an increase of 196% compared to the sample without adhesive. The shear and tensile strengths of the samples containing cellulose-based powder adhesive as an overlay are given in Table 9. The shear strength of the optimum specimen containing cellulose-based adhesive mortar (NWPH) was 10 % lower than the specimen without cellulose adhesive, which can be attributed to the loss of significant effect of wire brush roughness on adhesion resistance. It can also be seen that the tensile strength of the NWPH was lower than the specimen without HEMC, although the reduction was not significant.

Table 8. Average bond strength of composite specimens containing epoxy adhesive as a bonding agent.

Test type	Strength (MPa)	SD (MPa)	COV (%)
Shear test	4.05	0.34	8.4
Splitting tensile test	2.87	0.055	1.85

Note: SD – standard deviation, COV – coefficient of variance.

Table 9. Average bond strength of composite specimens containing HEMC mortar as a bonding agent.

Test type	Strength (MPa)	SD (MPa)	COV (%)
Shear test	1.61	0.071	4.40
Splitting tensile test	0.96	0.047	4.99

Note: SD – standard deviation, COV – coefficient of variance.

3.3. Failure modes

The failure modes of concrete materials without adhesive are shown in Fig. 10. Based on Figs. 10a-10c, the location of the failure plane of the NLN, NWN, and NSN composite specimens observed in the bi-surface shear test, one can deduce that cracks initiated from the top of the bond line and then propagated through the bottom of the specimen. When the load exceeded a specific value, sudden slippage occurred between the two concrete materials. It can be concluded that modes of fracture for all the specimens were adhesive failure, indicating the complete separation of the overlay concrete from the substrate, and the surfaces of the two materials remained smooth, and no further cracking was observed in both substrate and overlay.

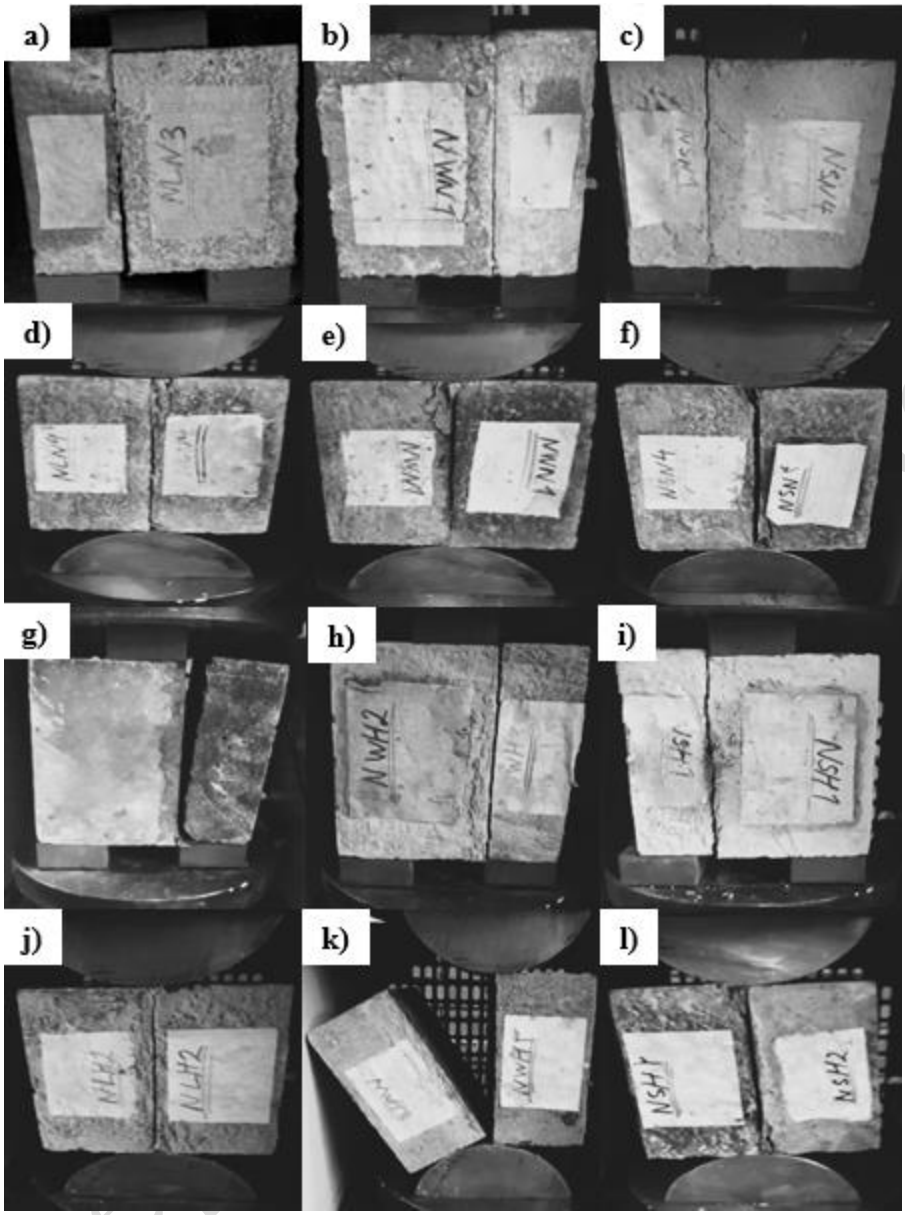

Fig. 10. The shear and tensile failure between two concrete materials: NSC-NSC and NSC-HSC.

Figs. 10d-10f demonstrate the tensile failure of the specimens containing NSC overlay. The failure in tension is similar to the failure in shear. In other words, the specimens had interface fractures, and no damage was observed either from the substrate or the overlay concrete. The crack in the specimens subjected to tension emerged from the middle of the interface and propagated on both sides until it reached the top and bottom of the specimen, and total failure of the specimens occurred. The failure modes of the specimens

containing HSC as an overlay, evaluated by bi-surface shear and tensile splitting tests, were all interfacial failures (Figs. 10g-10l). The interface failure indicates that the interfacial bond strength is weaker than the concrete substrate.

The complete separation of concrete surfaces in both shear and tensile stresses in interface failure is represented in Figs. 11a-11c. Fig. 11a demonstrates NSN specimens subjected to the splitting tensile test, in which a small portion of concrete was penetrated the hollows created by the chipping process, but the surface of concrete remained intact, and no further damage was observed on the surfaces. Fig. 11b shows the NWH specimen subjected to the bi-surface shear test. The interface failure mode occurred between the surfaces, similar to NSN samples. Fig. 11c also depicts the complete separation of NLH surfaces without harming either the substrate or the overlay concrete. Fig. 12a demonstrates the failure mode of the specimen containing epoxy adhesive under shear stress, and Fig. 12b demonstrates the failure mode of the specimen containing HEMC mortar at their interface that was subjected to tensile stress. Some specimens had mixed-mode failure, and some had interface failure. In other words, minor substrate failure and interface failure occurred in some specimens containing epoxy adhesive and HEMC as binding materials.

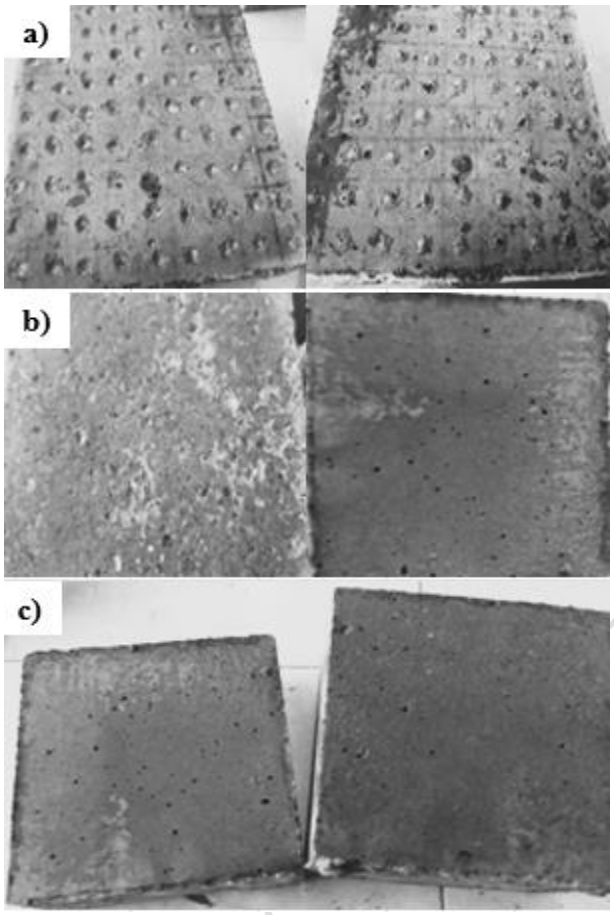

Fig. 11. The surfaces of the composites after failure in shear and tension (NSC-HSC): (a) NSN specimen subjected to the splitting tensile test; (b) NWH specimen subjected to the bi-surface shear test; (c) NLH specimen subjected to the splitting tensile test.

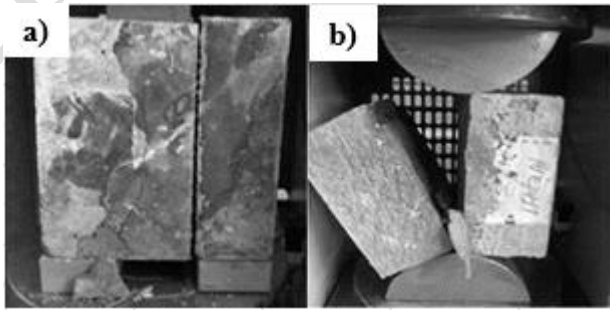

Fig. 12. The shear and tensile failure of the specimens: (a) epoxy-contained specimen; (b) HEMC-contained specimen.

Almost the total failure plane in shear and tension, originated from the interaction between the concrete substrate and the epoxy adhesive, not the epoxy adhesive itself (Fig. 13a & Fig. 13b). The same conclusion can be made for the HEMC specimens (Fig. 13c & Fig. 13d). In some of the specimens, the bond strength was distinctively stronger than that of the substrate because a failure occurred partially in the substrate without complete interfacial separation or debonding between the substrate and the overlay concrete. The failure from the concrete substrate highlights a good bond proficiency, indicating that the interfacial bond strength is more significant than the concrete substrate strength.

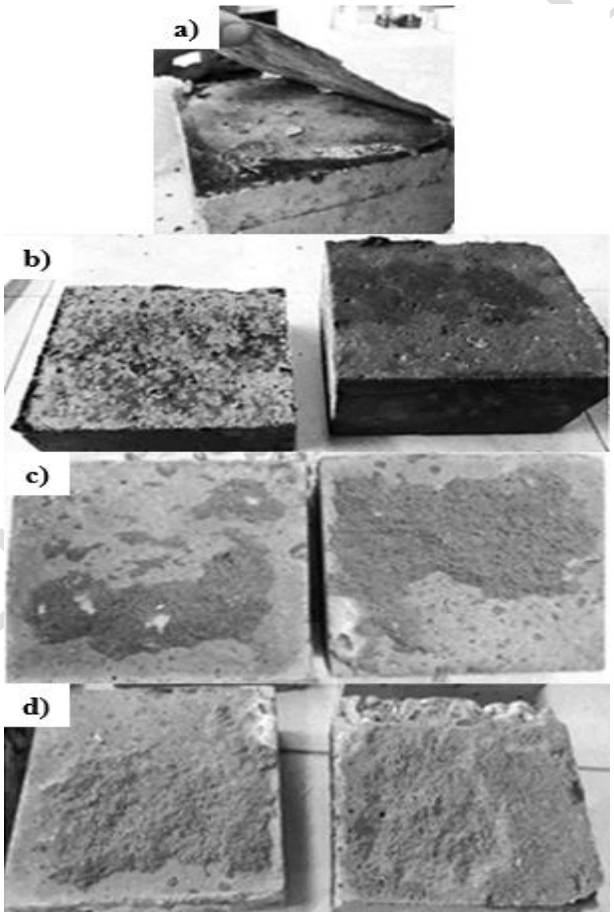

Fig. 13. The separation of concrete surfaces in shear and tension: (a, b) epoxy-contained specimen; (c, d) HEMC-contained specimen

4. Conclusions

The purpose of this study was to investigate the bonding strength behavior between two concrete materials by considering different parameters. To this end, the roughness parameters of the substrate concrete, including smooth surface, wire-brushed surface, and chipped surface, were examined, and the compressive strength of new concrete with two strength classes of 40 MPa and 70 MPa was evaluated separately by bi-surface shear and tensile splitting tests. Then the sample with the highest shear and tensile strength was introduced as the optimum specimen. Finally, an epoxy-based bonding agent and cellulose-based mortar were applied to the sample, and their failure mode and bond strength were compared to the optimum specimen. The following conclusions can be drawn:

- Surface treatment has a high impact on the shear and tensile strength of concrete composites. The shear and tensile strength of the concrete with the wire-brushed surface are the highest among other treatment methods. The reason was the mechanical interlocking between old concrete's exposed aggregates and overlay concrete's cement paste caused by wire-brushing. The shear and tensile strength of the composite specimens roughened by chipping was less than those roughened by the wire-brushed method. The reason behind this was the propagation of micro-cracks on the concrete substrate. Using high-strength concrete as an overlay material caused an increment in shear and tensile bond strength. The reason was due to the inclusion of micro silica in overlay concrete mix-proportion, which fills small voids at the interfacial zone and thus enhances adhesion and bonding strength.
- Shear and tensile strength of optimum design increased by adding epoxy adhesive between layers due to its strong

adhesion and chemical forces between concrete and the epoxy itself.

- The shear and tensile strength of the optimum design with cellulose-based adhesive mortar was less than the optimum specimen without cellulose mortar due to having a large thickness and the loss of roughness effect and in the concrete substrate. Due to conflicting results obtained from compressive and tensile strength tests, it cannot be definitely concluded that the other reason is the low mechanical performance of HEMC mortar.

References

Al-Osta, M.A., Ahmad, S., Al-Madani, M.K., Khalid, H.R., Al-Huri, M., Al-Fakih, A. (2022). "Performance of bond strength between ultra-high-performance concrete and concrete substrates (concrete screed and self-compacted concrete): An experimental study", *J. Build. Eng.* vol. 51, no. March (2022), 104291, https://doi.org/10.1016/j.jobe.2022.104291.

American Concrete Institute: Farmington Hills, MI. 1987.4. *ACI Committee 213:Guide for structural light-weight aggregate concrete (ACI 213R-87).*

Austin, S., Peter, R. and Youguang P. (1995). "Tensile bond testing of concrete repairs", *Materials and structures*, 28: 249-59.

Babafemi, A.J., Temitope K., Miah, Md.J., Paul, S.C. and Panda, B. (2021). "A concise review on interlayer bond strength in 3D concrete printing", *Sustainability*, 13: 7137.

Baharuddin, N.K., Fadzli M.N., Badorul Hisham, A.B., Salmia B. and A Tayeh, B. (2020). "Potential use of ultra high-performance fibre-reinforced concrete as a repair material for fire-damaged concrete in terms of bond strength", *International Journal of Integrated Engineering*, 12: 87-95.

Baloch, W.L., Hocine, S., Mohamed L. and Mustafa, S. (2021). "A review on the durability of concrete-to-concrete bond in recent rehabilitated structures", *Journal of Building Engineering*, 44: 103315.

Behforouz, B., Tavakoli, D,. Gharghani, M., Ashour, A. (2023). "Bond strength of the interface between concrete substrate and overlay concrete containing fly ash exposed to high temperature", *Structures* 49 (2023) 183–197, https://doi.org/10.1016/j.istruc.2023.01.122.

Beushausen, H., Björn, H. and Marco T. (2017). "The influence of substrate moisture preparation on bond strength of concrete overlays and the microstructure of the OTZ", *Cement and concrete research*, 92: 84-91.

BSI. 2000. "BS EN 12390-6: 2000: *Testing hardened concrete–tensile splitting strength of test specimens*. In.: BSI London, UK.

Bülichen, D., Kainz, J. and Plank, J. (2012). "Working mechanism of methyl hydroxyethyl cellulose (MHEC) as

water retention agent", *Cement and concrete research*, 42: 953-59.

Carbonell Muñoz, M.A., K Harris, D., Ahlborn, T.M. and C Froster D. (2014). "Bond performance between ultrahigh-performance concrete and normal-strength concrete", *Journal of Materials in Civil Engineering*, 26: 04014031.

Çolak, A., Turgay, Ç. and E Bakırcı, A. (2009). "Effects of environmental factors on the adhesion and durability characteristics of epoxy-bonded concrete prisms", *Construction and Building Materials*, 23: 758-67.

Courard, L., Piotrowski, T. and Garbacz A. (2014). "Near-to-surface properties affecting bond strength in concrete repair", *Cement and Concrete Composites*, 46: 73-80.

Daneshvar, D., Behnood A. and Robisson, A. (2022). "Interfacial bond in concrete-to-concrete composites: A review", *Construction and Building Materials*, 359: 129195.

de la Precontrainte, Federation Internationale. (1983). *FIP manual of lightweight aggregate concrete* (Surrey University Press).

Delor-Jestin, F., Drouin, D., Cheval, P-Y. and Lacoste, J. (2006). "Thermal and photochemical ageing of epoxy resin–Influence of curing agents", *Polymer Degradation and Stability*, 91: 1247-55.

Diab, A.M., Elmoaty, M.A. and Tag Eldin, M.R. (2017). "Slant shear bond strength between self compacting concrete and old concrete", *Construction and Building Materials*, 130: 73-82.

Du, Wei., Yu, J., Gu, Y., Li, L., Han, X. and Liu, Q. (2019). "Preparation and application of microcapsules containing toluene-di-isocyanate for self-healing of concrete", *Construction and Building Materials*, 202: 762-69.

Dybeł, P. and Wałach, D. (2017). "Evaluation of the development of bond strength between two concrete layers", *IOP Conference Series: Materials Science and Engineering*, 032056. IOP Publishing.

EL Afandi, M., Yehia, S., Landolsi, T., Qaddoumi, N., Elchalakani, M. (2023). "Concrete-to-concrete bond Strength: A review", *Constr. Build.Mater*, 363, 129820.

EN, British Standard. (2009). *Testing hardened concrete–Part 3: Compressive strength of test specimens*. British Standard Institution, London, UK.

Ezoddin, A., Kheyroddin,. A. and Gholhaki, M. (2020). "Investigation of the Effects of Link Beam Length on the RC Frame Retrofitted with the Linked Column Frame System", *Civil Engineering Infrastructures Journal*, 53: 137-59.

Farzad, M., Shafieifar, M. and Azizinamini, A. (2019). "Experimental and numerical study on bond strength between conventional concrete and Ultra High-Performance Concrete (UHPC)", *Engineering Structures*, 186: 297-305.

Feng, S., Xiao, H. and Li, H. (2020). "Comparative studies of the effect of ultrahigh-performance concrete and normal concrete as repair materials on interfacial bond properties and microstructure", *Engineering Structures*, 222: 111122.

Feng, S., Xiao, H., Liu, R. and Liu, M. (2022). "The bond properties between ultra-high-performance concrete and normal strength concrete substrate: Bond macro-performance and overlay transition zone

microstructure", *Cement and Concrete Composites*, 128: 104436.

Gadri, K. and Guettala, A. (2017). "Evaluation of bond strength between sand concrete as new repair material and ordinary concrete substrate (The surface roughness effect)", *Construction and Building Materials*, 157: 1133-44.

Guo, T., Xie, Y. and Weng, X. (2018). "Evaluation of the bond strength of a novel concrete for rapid patch repair of pavements", *Construction and Building Materials*, 186: 790-800.

He, Y., Zhang, X., Hooton, R.D. and Zhang, X. (2017). "Effects of interface roughness and interface adhesion on new-to-old concrete bonding", *Construction and Building Materials*, 151: 582-90.

Huang, H., Yuan, Y., Zhang, W. and Gao, Z. (2019). "Bond behavior between lightweight aggregate concrete and normal weight concrete based on splitting-tensile test", *Construction and Building Materials*, 209: 306-14.

Jafarinejad, S., Rabiee, A., Shekarchi, M. (2019). "Experimental investigation on the bond strength between Ultra high strength Fiber Reinforced Cementitious Mortar and conventional concrete", *Constr. Build. Mater.* 229 (2019), 116814, https://doi.org/ 10.1016/j.conbuildmat.2019.116814.

Julio, E. NBS., AB Branco, F. and. D Silva, V. (2004). "Concrete-to-concrete bond strength. Influence of the roughness of the substrate surface", *Construction and Building Materials*, 18: 675-81.

Julio, E.NBS., Fernando, AB Branco., D Silva, V. and Lourenço. J.F. (2006). "Influence of added concrete compressive strength on adhesion to an existing concrete substrate", *Building and Environment*, 41: 1934-39.

Mangat, P.S. and O'Flaherty, F.J. (2000). "Influence of elastic modulus on stress redistribution and cracking in repair patches", *Cement and concrete research*, 30: 125-36.

Michels, J., Sena Cruz, J.,Christen, R., Czaderski, C. and Motavalli, M. (2016). "Mechanical performance of cold-curing epoxy adhesives after different mixing and curing procedures", *Composites Part B: Engineering*, 98: 434-43.

Mizan, M.Ha., Ueda, T. and Matsumoto, K. (2020). "Enhancement of the concrete-PCM interfacial bonding strength using silica fume", *Construction and Building Materials*, 259: 119774.

Momayez, A., Ehsani M.R., Ramezanianpour A.A. and Rajaie, H. (2005). "Comparison of methods for evaluating bond strength between concrete substrate and repair materials", *Cement and concrete research*, 35: 748-57.

Nawy, E.G. (2000). *Fundamentals of high-performance concrete* (John Wiley & Sons).

Pourchez, J., Peschard, A., Grosseau, P., Guyonnet, R., Guilhot, B. and Vallée, F. (2006). "HPMC and HEMC influence on cement hydration", *Cement and concrete research*, 36: 288-94.

Prado, L.P., Carrazedo, R. and El Debs, M.K. (2022). "Interface strength of High-Strength concrete to Ultra-High-Performance concrete", *Engineering Structures*, 252: 113591.

Santos, D., M.D Santos, P. and Dias-da-Costa, D. (2012). "Effect of surface preparation and bonding agent on the concrete-to-concrete interface

strength", *Construction and Building Materials*, 37: 102-10.

Shibao, H., Mizan, M.H., Ueda, T., Miyaguchi, K. and Takahashi, J. (2019). "A study on effect of silica fume and surface penetrant on bonding strength for overlaying", *Journal of Asian Concrete Federation*, 5: 1-14.

Shin, A.H. and A Lange, D. (2012). "Effects of overlay thickness on surface cracking and debonding in bonded concrete overlays", *Canadian journal of civil engineering*, 39: 304-12.

Tayeh, B.A., Abu Bakar, Megat Johari, M.A. and Voo, Y.L. (2012). "Mechanical and permeability properties of the interface between normal concrete substrate and ultra high performance fiber concrete overlay", *Construction and Building Materials*, 36: 538-48.

Tu, T., Chen, Y. and Hwang, C. (2006). "Properties of HPC with recycled aggregates", *Cement and concrete research*, 36: 943-50.

Valikhani, A., Jaberi Jahromi, A., Mantawy I. and Azizinamini, A. (2020). "Experimental evaluation of concrete-to-UHPC bond strength with correlation to surface roughness for repair application", *Construction and Building Materials*, 238: 117753.

Valipour, M. and Khayat K.H. (2020). "Debonding test method to evaluate bond strength between UHPC and concrete substrate", *Materials and structures*, 53: 1-10.

Xu, J. and Hao, P. (2012). "Study of aggregate gradations in foamed bitumen mixes", *Road materials and pavement design*, 13: 660-77.

Zhou, J., Ye, G., Schlangen, E. and Breugel, K. (2008). "Modelling of stresses and strains in bonded concrete overlays subjected to differential volume changes", *Theoretical and Applied Fracture Mechanics*, 49: 199-205.